

# HAZARD ANALYSES OF GLINT AND GLARE FROM CONCENTRATING SOLAR POWER PLANTS

**Clifford K. Ho<sup>1</sup>, Cheryl M. Ghanbari<sup>2</sup>, and Richard B. Diver, Jr.<sup>2</sup>**

<sup>1</sup>Ph.D., Sandia National Laboratories, Solar Technologies Department, P.O. Box 5800, Albuquerque, NM 87185-1127, USA  
Phone: 1-505-844-2384, E-mail: [ckho@sandia.gov](mailto:ckho@sandia.gov)

<sup>2</sup>Test Engineer, Sandia National Laboratories, Solar Technologies Department

<sup>3</sup>Ph.D., Sandia National Laboratories, Solar Technologies Department

## Abstract

Glint and glare from concentrating solar collectors and receivers may pose a potential hazard or distraction for motorists, pilots, and pedestrians. This paper provides analytical and computational methods to evaluate the irradiance originating from specularly and diffusely reflecting sources as a function of distance and characteristics of the source. Sample problems are provided for both specular and diffuse sources. In addition, a review of the physiology, optics, and damage mechanisms associated with ocular radiation is provided. A summary of safety metrics and standards is also compiled from the literature to evaluate the potential hazards of calculated irradiances from glint and glare. Previous safety metrics have focused on prevention of permanent eye damage (e.g., retinal burn). New metrics are introduced in this paper for temporary flash blindness, which can occur at irradiance values several orders of magnitude lower than the irradiance values required for irreversible eye damage.

## 1. Introduction

Assessment of the potential hazards of glint and glare from solar thermal power plants is an important requirement to ensure public safety. Glint is defined as a momentary flash of light, while glare is defined as a more continuous source of excessive brightness relative to the ambient lighting. Hazards from glint and glare from solar thermal power plants include the potential for permanent eye injury (e.g., retinal burn) and temporary distractions (e.g., flash blindness). Distractions from glint or glare can be hazardous to pilots flying overhead or to motorists driving alongside the site.

Applications and certifications for solar thermal power plants often require an assessment of “visual resources” at the site, but these requirements typically focus on aesthetic qualities and standards. Certifications also require an evaluation of general health and safety issues associated with the site, but rigorous and uniform treatment of glint and glare are lacking. The purpose of this paper is to summarize previous analyses and provide general assessment methods that can be used to evaluate potential hazards of glint and glare for all of the primary concentrating solar power (CSP) technologies: (1) power tower systems, (2) linear concentrator systems (e.g., parabolic troughs), and (3) dish/engine systems.

## 2. Review of Previous Assessments

The following sections summarize previous assessments that were conducted to evaluate potential glint and glare hazards from power towers, linear receivers, and dish collector systems. Figure 1, Figure 2, and Figure 3 show photographs of observed specular and diffuse reflections from these different types of systems.

### 2.1 Power Towers

Brumleve [1],[2] provided some of the earliest analyses of eye hazards associated with central receiver technologies. Analytical models were developed to assess light intensities and hazardous ranges of single and multiple coincident heliostat beams at ground level and in the air space above a central receiver facility at Sandia National Laboratories in Albuquerque, New Mexico. Distances were calculated to ensure safe retinal irradiance levels (based on work from Sliney and Freasier [3]), and results showed that retinal

irradiance from single heliostat beams exceeded the safe limits only within a short range (up to 40 m) within the focal distance of the heliostat. For heliostats with focal distances greater than 270 m, the safe retinal limits were never exceeded. The safe number of multiple coincident beams was also calculated as a function of distance, focal length, and projected area density. Based on these analyses, exclusion zones (restricted areas) and beam control techniques were recommended to minimize the potential hazards from single and multiple heliostat beams during operation.

Brumleve [2] also used video techniques during helicopter flyovers and at ground level to determine retinal irradiance, image size, and receiver brightness for the 10 MW<sub>e</sub> solar thermal central receiver pilot plant in Barstow, California. Safe limits were not exceeded in the airspace above an altitude of ~240 m, which is the lowest allowable altitude for aircraft near the 91-m tall receiver tower. It was also found that the receiver was not bright enough to constitute an eye hazard during momentary viewing.

The probability of multiple heliostat beams randomly crossing in the airspace above the proposed Ivanpah Solar Electric Generating System in California was calculated in an application submitted to the California Energy Commission [4]. They showed that the probability of a sufficient number of heliostat beams (8) crossing at the same point to exceed safety limits at an altitude of 1000 m was infinitesimally small.



Figure 1. Specular reflections from heliostats at Solar One (10 MW<sub>e</sub> Power Tower, Daggett, CA).

## 2.2 Linear Receivers

Glint and glare analyses have been performed for the proposed Carrizo Energy Solar Farm in San Luis Obispo County, California, which consists of nearly 200 lines of compact linear Fresnel reflector systems [5]. Diffuse reflection from the receiver pipes and spillage intensity from the reflectors were evaluated. Results showed that unsafe beam intensities could be posed to pedestrians within ~18 m of the perimeter fence; therefore, privacy slats in the perimeter fence were proposed. Other scenarios associated with reflected light were not found to be likely hazards.

An application for certification of the Victorville 2 Hybrid power Project [6] included a letter from the California Department of Transportation, Division of Aeronautics, that conducted flyovers of existing parabolic trough plants at Kramer Junction and Harper Lake in Southern California. The glare and flash was found to be similar to the reflection over a smooth water surface. In addition, a letter from the chief operating officer of the Kramer Junction facility stated that the observed reflections originated primarily from the receiver tubes and that the glare has not been a distraction to pilots in nearly 20 years of operation.

A recent application for certification of the San Joaquin Solar 1 & 2 project submitted to the California Energy commission included a glint and glare analysis for their proposed parabolic trough plant [7]. The

analysis evaluated the diffuse reflection from the receiver pipes (heat collection elements), and they concluded that the diffusely reflected sunlight from the receiver pipes would be 150 times less than the intensity of the sun and therefore not a hazard. The beam intensity caused by specular reflection from the mirrors was also considered to evaluate potential glare when the parabolic troughs were being rotated from stow position to tracking position. Results showed that the beam intensity could be unsafe for pedestrians within 60 feet from the plant perimeter (although details of the calculations and metrics were not provided), so privacy slats in the perimeter fence were recommended.



Figure 2. Specular and diffuse reflections from receiver tube at Kramer Junction (150 MW<sub>e</sub> Parabolic Trough, Mojave Desert, CA).

### 2.3 Dish/Engines

A qualitative glint and glare analysis of dish/engine systems for the SES Solar Two Project was conducted as part of the application for certification that claimed that distracting, blinding, or hazardous glint or glare effects should not be a problem [8]. However, detailed analyses of the potential for hazardous reflections during off-axis positions (e.g., during stowing, start-up, or abnormal operations) was not performed.

Ghanbari and Diver [9] developed a mathematical model to investigate the maximum viewing time of diffuse reflections from a dish receiver aperture plate (see Appendix). The maximum viewing time was based on exposure limits for optical radiation published by the American Conference of Governmental Industrial Hygienists (ACGIH) [10]. Their results showed that diffusely reflected radiation from the receiver did not pose hazards for retinal thermal damage, retinal photochemical injury, and infrared radiation damage.

In 1980, Sliney evaluated hazards of the reflected sunlight from the point-focus collectors at the JPL/Edwards test site [11]. He first analyzed the hazards from viewing the sun directly and concluded that the natural blink response of 0.1 – 0.2 seconds is adequate to protect viewers from thermal retinal and photochemical injury. However, prolonged staring at the sun when it is high in the sky or viewing it, unfiltered, through a magnifier such as binoculars or telescopes will result in thermal retinal damage. He then analyzed viewing of reflected sunlight from a point-focus collector. Sliney concluded that if an observer is less than one focal length away from a single facet on a point-focus collector, even for short exposures, injury could occur. However, when a dish is tracking the sun, it is virtually impossible for anyone, worker or observer, to be less than one focal length for any one facet. The situation that is of greater concern is when the dish is not tracking the sun but is in an off-axis position that could still reflect sunlight onto a worker or observer. In these cases, however, the reflected sunlight would not emanate from the entire dish, but rather from an individual facet, and observers would not be exposed to reflections that are more dangerous than the sun itself.



Figure 3. Specular reflections from stowed parabolic dish collectors at National Solar Thermal Test Facility, Sandia National Laboratories, NM.

#### 2.4 Discussion of Previous Analyses

In the previous analyses of glint and glare for concentrating solar thermal power plants, permanent eye damage was used as the metric to determine safe retinal irradiance values. The safe retinal irradiance thresholds were based on retinal burn tests performed on rabbits [3]. In the next section, additional metrics are discussed, including temporary flash blindness. Data from past research on flash blindness and recovery times from after-image disability are reviewed to provide additional quantitative metrics that may be used for glint and glare evaluations of concentrating solar thermal power plants.

### 3. Ocular Irradiation and Safety Metrics

#### 3.1 Anatomy of the Eye

Figure 4 shows an illustration of the human eye and how an image is projected onto the retina. Light rays enter through the cornea and pass through the pupil, which can vary in aperture size from 2 – 3 mm for a sunlight-adapted eye to 7 – 8 mm for a dark-adapted eye. The rays pass through the lens and converge at a nodal point behind the lens. The image is then inverted and projected onto the retina, a distance approximately 1.7 cm behind the nodal point in healthy eyes.

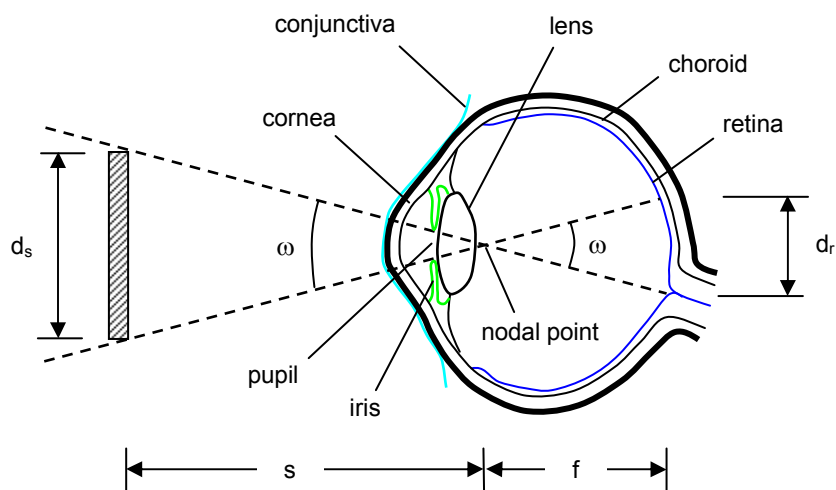


Figure 4. Image projected onto the retina of a human eye.

Potential damage to the eye depends on a number of factors including the source radiance, source angle (size and distance to eye), duration of exposure, and wavelength. The spectral distribution of sunlight is heavily weighted in the visible bandwidth (400 – 700 nm), but the eye can pass wavelengths between 400 and 1400 nm to the retina. The lens of the eye is a strong absorber of wavelengths less than 400 nm [3]. At lower wavelengths, UV-B and UV-C radiation are absorbed in the cornea and conjunctiva, and sufficient doses can cause keratoconjunctivitis (welder's flash) and photokeratitis (snow blindness) [3],[12]. Solar retinitis and eclipse blindness are caused primarily by photochemical damage (rather than thermal injury) in the visible spectrum between 380 and 580 nm. Between 580 and 1400 nm, photothermal damage predominates over photochemical damage. Because the blink response of the eye is rapid (0.15 – 0.2 s) [3], exposure to reflected sunlight is expected to be short in duration.

### 3.2 Retinal Irradiance

The retinal irradiance (power per unit area) can be calculated from the total power entering the pupil and the retinal image area. The area projected onto the retina (assuming circular images) can be determined from the source angle ( $\omega$ ), which can be calculated from the source size ( $d_s$ ) and distance ( $s$ ), and the focal length ( $f$ ), as follows (refer to Figure 4):

$$d_r = f \omega \quad (1)$$

where  $\omega = d_s / s$

Eq. (1) assumes that the arc and the chord of a circle are the same for small angles. At a source angle,  $\omega$ , of 60°, the error in  $d_r$  is ~5%. If the irradiance at a plane in front of the cornea,  $E_c$  (W/m<sup>2</sup>), is known, the power entering the pupil can be calculated as the product of the irradiance and the pupil area (the diameter of the pupil,  $d_p$ , adjusted to sunlight is ~2 mm). The power is then divided by the retinal image area and multiplied by a transmission coefficient,  $\tau$  (~0.5 [11]), for the ocular media (to account for absorption of radiation within the eye before it reaches the retina) to yield the following expression for the retinal irradiance:

$$E_r = E_c \left( \frac{d_p^2}{d_r^2} \right) \tau \quad (2)$$

If the source radiance,  $L$  (W/m<sup>2</sup>/sr) is known, the corneal irradiance in Eq. (2) can be determined by multiplying the radiance by the subtended solid angle of the source,  $\Omega$  (sr):

$$E_c = L \Omega = L \frac{A_s}{s^2} \approx L \left( \frac{\pi}{4} \omega^2 \right) \quad (3)$$

and the retinal irradiance can be calculated directly from the radiance as follows:

$$E_r = \frac{\pi L \tau}{4} \left( \frac{d_p}{f} \right)^2 \quad (4)$$

It should be noted that Brumleve [1] includes an additional coefficient ( $v$ ) to account for the fraction of solar irradiance between 400 and 1400 nm, but this has been included in the transmission coefficient,  $\tau$ , above. As an example, the retinal irradiance caused by viewing the sun directly can be calculated using Eqs. (1) and (2) with  $E_c = 0.1$  W/cm<sup>2</sup>,  $d_p = 0.002$  m,  $f = 0.017$  m,  $\omega = 0.0093$  rad, and  $\tau = 0.5$ , which yields a retinal irradiance,  $E_r$ , of ~8 W/cm<sup>2</sup>. Note that the retinal irradiance is significantly higher than the irradiance at the entrance of the eye. For applications involving images of the sun, the retinal irradiance can be converted to corneal irradiance using Eqs. (1) and (2) with  $d_p = 0.002$  m,  $f = 0.017$  m,  $\omega = 0.0093$  rad (sun shape), and  $\tau = 0.5$ , yielding the following approximate relation:  $E_c = 0.0125 E_r$ .

### 3.3 Safety Metrics

Safety metrics relevant to optical radiation and the prevention of permanent eye damage are reviewed and presented in this section. In addition, previous studies pertaining to flash blindness are also presented since

temporary flash blindness is potentially hazardous to motorists or pilots. Other consequences from glint and glare such as discomfort and distraction have been evaluated in the literature [13],[14], but the subjective impacts of discomfort and distraction glare are not considered in this paper.

### 3.3.1 Safe Retinal Irradiance Values from Retinal Burn Data

Sliney and Freasier [3] presented maximum permissible retinal irradiance levels ( $\text{W}/\text{cm}^2$ ) based on retinal burn data using rabbits. Brumleve [1] used this data to develop a convenient metric for safe retinal irradiance,  $E_{rs}$  ( $\text{W}/\text{cm}^2$ ) based on retinal image size,  $d_r$  (m), assuming circular images and a 0.15 second exposure (typical blink response):

$$E_{rs} = \begin{cases} \frac{0.002}{d_r} & \text{for } d_r < 0.002 \text{ m} \\ 1 & \text{for } d_r \geq 0.002 \text{ m} \end{cases} \quad (5)$$

Eq. (5) has been used by several analyses of glint and glare for concentrating solar thermal power plants [4],[5],[7]. However, the calculated safe retinal irradiance value that was used in these analyses is based on specific properties of a heliostat (e.g., reflectivity, beam divergence) reported by Brumleve [2] that may not be generally applicable to other collector systems. The safe retinal irradiance value for viewing the sun directly can be calculated using Eq. (5) and the subtended angle of the sun (~9.3 mrad) to calculate the retinal image diameter. The safe retinal irradiance value is 12.7  $\text{W}/\text{cm}^2$ , which is about 1.6 times greater than the retinal irradiance experienced from viewing the sun directly (~8  $\text{W}/\text{cm}^2$ ). Note that the retinal irradiance is greater than the corneal irradiance (or “irradiance at the eye”) because of the smaller image area projected onto the retina (relative to the pupil size). The equivalent safe corneal irradiance for a subtended angle of 9.3 mrad is 0.16  $\text{W}/\text{cm}^2$  or 1600  $\text{W}/\text{m}^2$ .

### 3.3.2 ANSI 2000 Standard

More recently, Delori et al. [15] provide a concise formulation and summary of the American National Standards Institute (ANSI) Z136.1-2000 Standard for the protection of the human eye from laser exposure. They note that the recommended exposure limits for lasers and broadband sources (such as the sun) are not substantially different. Delori et al. [15] present maximum permissible power levels entering the pupil as a function of exposure duration, wavelength, and source angle. For brief exposures (0.15 – 0.2 s), Table 3 in Delori et al. [15] provides the following expression for the maximum permissible power level,  $MP$  (W):

$$MP = 6.93 \times 10^{-4} C_T C_E P^1 t^{0.25} \quad (6)$$

where  $C_T$  is a function of wavelength (ranges between 1 and 40 at wavelengths between 400 and 1400 nm),  $C_E$  is a function of the source angle (6.2 for an angle of 9.3 mrad subtended by the sun),  $P$  is a pupil factor that is a function of exposure time and wavelength (ranges between 1.8 and ~1 for wavelengths between 400 and 1400 nm), and  $t$  is the exposure time (s). Using solar-radiance spectrally weighted values for the coefficients provided by Delori et al. [15] and an assumed exposure duration of 0.15 seconds yields a maximum permissible power at the pupil of ~0.008 W and maximum retinal irradiance of ~40  $\text{W}/\text{cm}^2$  (which corresponds to a safe corneal irradiance of ~0.5  $\text{W}/\text{cm}^2$  or 5000  $\text{W}/\text{m}^2$ ). This value is about three times greater than the values proposed by Brumleve [1],[2]. The difference is probably due to several factors including the use of different factors of safety (up to an order of magnitude or more) in the calculations.

### 3.3.3 ACGIH Threshold Limit Values

Spectrally weighted exposure limits for optical radiation have also been published by the American Conference of Governmental Industrial Hygienist (ACGIH) [10]. These limits are called Threshold Limit Values (TLVs) and are calculated from spectrally weighted radiometric values of radiance or irradiance. TLVs are evaluated for (1) retinal thermal damage, (2) photochemical injury from chronic blue light exposure, (3) and infrared radiation damage. The Appendix contains more details regarding these TLVs and

sample calculations.

### 3.3.4 Flash Blindness

Flash blindness results from bleaching of retinal visual pigments caused by bright (high luminance) sources of light. Photometric units are used to characterize the levels of brightness (or luminance) ( $\text{lumens}/\text{m}^2/\text{sr}$ ) or illuminance ( $\text{lumens}/\text{m}^2$ ) that cause flash blindness. Most people have experienced flash blindness after viewing a flash bulb from a camera or a bright light in a darkened room. A number of tests were performed by the U.S. Air Force to assess the visual recovery times for individuals exposed to bright flashes of light, primarily to determine how long it would take for pilots to read their instrument panels after being exposed to illumination from nuclear blasts [16],[17]. These studies found that visual recovery times ranged from 4 – 12 seconds for illuminance values ranging from  $\sim 650$  –  $1,100 \text{ lumens}/\text{m}^2$ . For light emitted within the solar spectrum, this corresponds to approximately  $7$  –  $11 \text{ W}/\text{m}^2$  of solar irradiance at the eye.

Additional tests were performed by Saur and Dobrash [18] to determine visual recovery times of individuals after being exposed to simulated sun reflections. They found that recovery times ranged from 0.8 – 2.7 seconds for illuminance values ranging from  $120$  –  $280 \text{ lumens}/\text{m}^2$ . Based on the solar spectrum, this is equivalent to approximately  $1$  –  $3 \text{ W}/\text{m}^2$  of solar irradiance at the eye.

From these data, it appears that a solar irradiance on the order of  $1 \text{ W}/\text{m}^2$  or  $1 \times 10^{-4} \text{ W}/\text{cm}^2$  at the eye is sufficient to cause temporary flash blindness. Assuming that this solar irradiance originates from an image that subtends a similar angle to the sun (9.3 mrad) with  $d_p = 0.002 \text{ m}$ ,  $f = 0.017 \text{ m}$ , and  $\tau = 0.5$ , the retinal irradiance that can cause flash blindness is  $\sim 8 \times 10^{-3} \text{ W}/\text{cm}^2$ . Comparing these solar irradiance values against the metrics used for calculating irreversible eye damage (e.g., Eqs. (5) or (6)) shows that flash blindness can occur at irradiances that are 2 – 3 orders of magnitude less than the irradiance metrics used for irreversible eye damage.

### 3.3.5 Summary of Safety Metrics

Figure 5 summarizes the safe irradiance values and flash blindness metrics discussed above for a 0.15 s exposure. As the subtended source angle increases, the safe retinal irradiance threshold decreases because of the increased size of the retinal image area, and, hence, increased energy applied to the retina. The metrics proposed by Brumleve [1] for safe retinal irradiances appear to be more conservative relative to the other standards plotted. The potential for flash blindness shown in the plot was based on an irradiance value of  $1 \times 10^{-4} \text{ W}/\text{cm}^2$  from the above studies, and the retinal irradiance was then determined using Eqs. (1) and (2) with  $d_p = 0.002 \text{ m}$ ,  $f = 0.017 \text{ m}$ , and  $\tau = 0.5$ . The plotted retinal irradiance values for potential flash blindness appear reasonable when compared to retinal irradiance values of several common sources of light reported by Sliney and Freasier [3]: incandescent bulb ( $\sim 10^{-4} \text{ W}/\text{cm}^2$ ), pyrotechnic flare ( $\sim 10^{-3} \text{ W}/\text{cm}^2$ ), tungsten filament ( $\sim 10^{-2} \text{ W}/\text{cm}^2$ ). Depending on the subtended source angle, the retinal irradiance that causes flash blindness can be 2 – 4 orders of magnitude less than the safe retinal irradiance metrics to prevent irreversible eye damage.

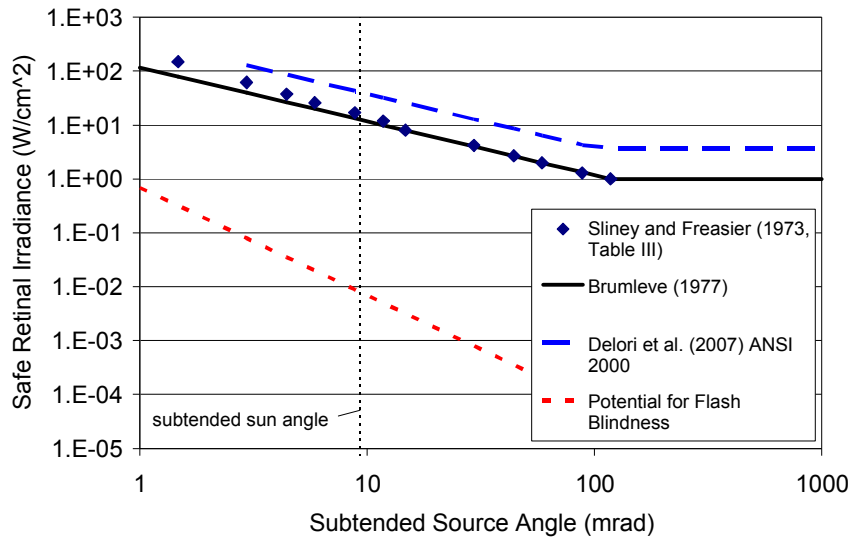


Figure 5. Safe retinal irradiance values as a function of subtended source angle for 0.15 s exposure (typical blink response time).

#### 4. Calculating Irradiance from Specular and Diffuse Reflections of Sunlight

This section presents analytical methods for calculating irradiance caused by specular and diffuse reflections of sunlight as a function of distance and other characteristics of the source. Specular reflections occur from polished mirror-like surfaces so that the reflected angle is equal to the incident angle relative to the surface normal. Diffuse reflections occur from uneven or rough surfaces that scatter the incident radiation uniformly in all directions (see Figure 6). The following sections provide methods to calculate the irradiance from specular and diffuse reflections. Once the irradiance is determined, the equations in the previous section can be used to calculate the retinal irradiance for comparison against the safe retinal irradiance metrics presented in Figure 5.

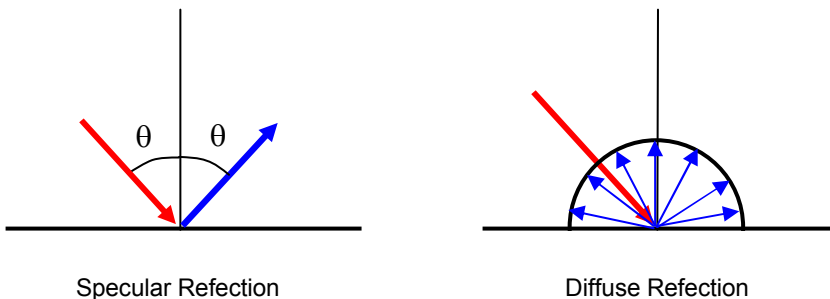


Figure 6. Illustration of specular versus diffuse reflections.

##### 4.1 Analytical Model of Specular Reflections

Direct specular solar reflection from mirrors can cause glint and glare hazards when heliostats are in standby positions (reflecting the sun at locations other than the receiver). Specular solar reflections from dishes and parabolic troughs can cause glint and glare hazards when the collectors are in off-axis positions (e.g., when moving from a stowed position to a tracking position). For parabolic troughs, glint and glare from specular reflections can also occur when the sun is low in the horizon and aligned with the axis of the trough, causing

reflected rays to spill from the end of the trough.

An analytical model of beam irradiance resulting from specular solar reflections from a focused mirror has been derived [1] with the following assumptions (see Figure 7):

- Uniform sun intensity (no limb darkening)
- Round, focused, continuous surface mirrors
- No cosine losses, off-axis aberrations, or atmospheric attenuation
- Uniform intensity in beam cross section

The assumptions above will generally produce the largest beam irradiance, but the assumption of uniform sun intensity averages the intensity over the entire beam. Using a non-uniform solar intensity creates larger peak fluxes towards the center of the beam. Comparisons with a ray-tracing model (ASAP<sup>®</sup>) show that the difference in peak flux is about 25-30% at the focal length, but the difference can be greater at other distances.

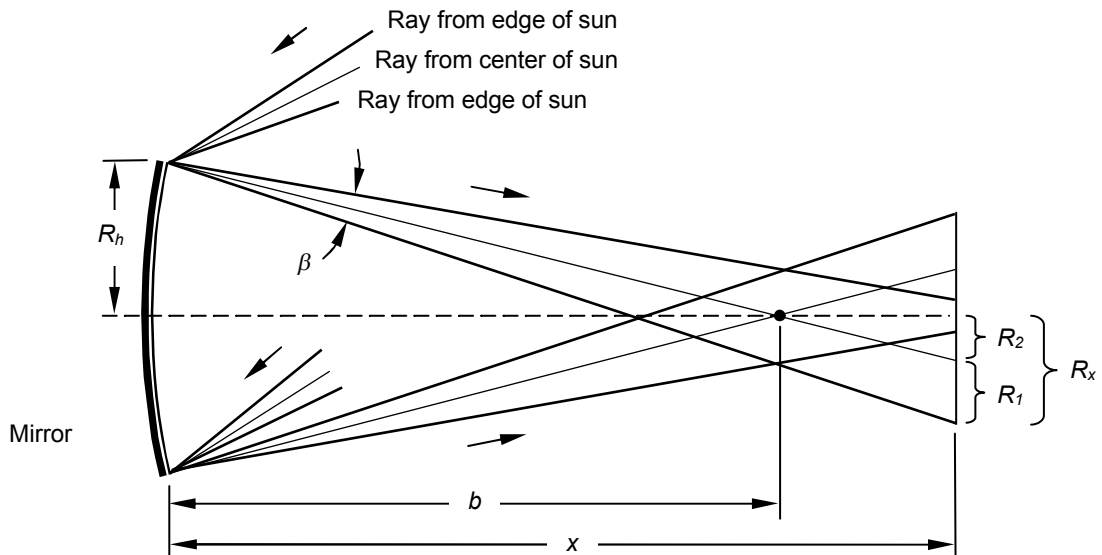


Figure 7. Geometry of specular solar reflections from a focused mirror where  $b$  is the focal length,  $R_h$  is the radius of the mirror,  $\beta$  is the beam divergence angle, and  $R_x$  is the radius of the beam cross section at distance,  $x$ , from the mirror (adapted from [1]).

The beam intensity,  $I$  [W/cm<sup>2</sup>], is then calculated as the product of the direct normal insolation,  $Q$  [W/cm<sup>2</sup>], the mirror reflectivity,  $\rho$  [-], and the area concentration ratio,  $C$  [-]:

$$I = \rho Q C \quad (7)$$

The direct normal insolation,  $Q$ , at the earth's surface is approximately 0.1 W/cm<sup>2</sup>. The area concentration ratio,  $C$ , can be calculated as follows assuming a circular mirror area,  $A_h$ , with radius,  $R_h$ , and a circular beam area,  $A_x$ , with radius,  $R_x$ , at a distance,  $x$ , from the mirror:

$$C = \frac{A_h}{A_x} = \left( \frac{R_h}{R_x} \right)^2 \quad (8)$$

The radius,  $R_x$ , of the beam is comprised of two components:

$$R_x = R_1 + R_2 \quad (9)$$

where  $R_1$  is caused by the sun angle and mirror contour inaccuracies (slope error) and  $R_2$  represents the

focusing and defocusing characteristics of the beam at a distance that is less than or greater than the focal length. The beam divergence,  $R_1$ , at a distance,  $x$ , from the mirror is defined by the sun half-angle (4.7 mrad) and any additional slope errors caused by mirror inaccuracies:

$$R_1 \approx x \tan\left(\frac{\beta}{2}\right) \quad (10)$$

where  $\beta/2$  is the half-angle [rad] of the total beam divergence. According to [1], this approximation has an error that is less than 0.3% for  $b/R_h > 18$ .  $R_2$  can be defined using similar triangles as shown in Figure 7, where  $b$  is the focal length:

$$\begin{aligned} \frac{R_2}{|x-b|} &= \frac{R_h}{b} \\ \Rightarrow R_2 &= \left| \frac{x}{b} - 1 \right| R_h \end{aligned} \quad (11)$$

Using Eqs. (8), (9), (10), and (11) in Eq. (7), and the approximation that  $\tan(\beta/2) = \beta/2$  when  $\beta/2$  is small, the following expression for the beam intensity [W/cm<sup>2</sup>] can be written:

$$I = \rho Q \left( \frac{x\beta}{D_h} + \left| \frac{x}{b} - 1 \right| \right)^{-2} \quad (12)$$

where  $D_h = 2 R_h$ . The beam intensity can also be presented in units of “suns” by dividing Eq. (12) by  $Q$  ( $\sim 0.1$  W/cm<sup>2</sup>). The maximum beam intensity occurs at the focal length,  $x = b$ . In addition, the beam intensity for a flat mirror can be calculated by setting  $b = \infty$  in Eq. (12). The beam intensity for several focal lengths is plotted in Figure 8 as a function of distance,  $x$ , from the mirror. The reflectivity,  $\rho$ , is assumed to be 0.92, and the total beam divergence angle,  $\beta$ , is assumed to be equal to 9.4 mrad. The effective diameter of the mirror,  $D_h$ , is calculated from the total mirrored area (37 m<sup>2</sup>) of individual heliostats used at the National Solar Thermal Test Facility at Sandia National Laboratories in Albuquerque, NM:

$$D_h = \left( \frac{4A_h}{\pi} \right)^{0.5} \quad (13)$$

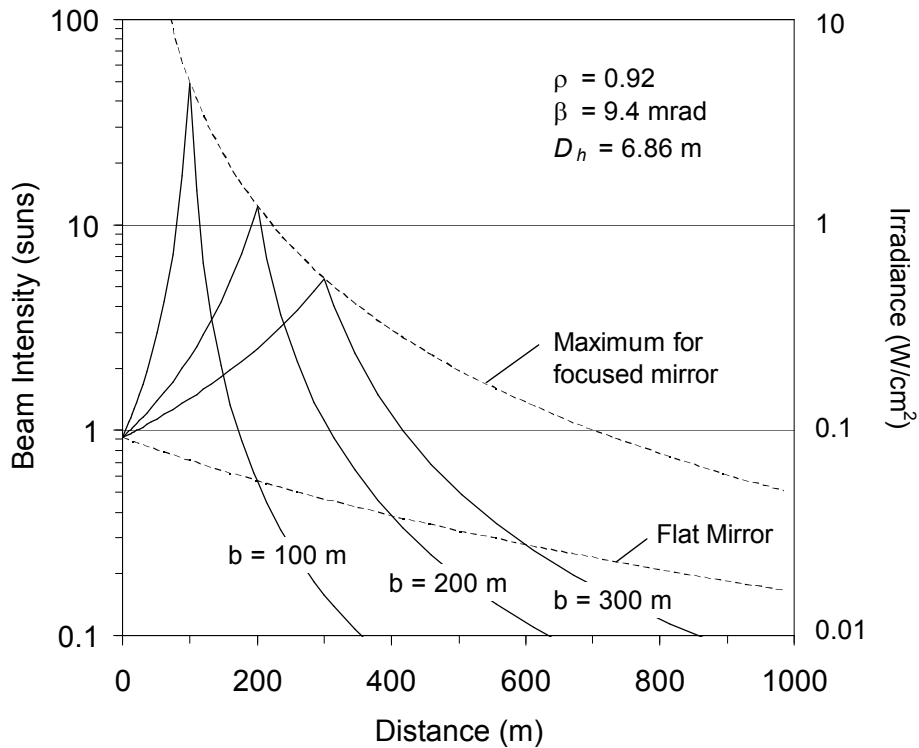


Figure 8. Plot of beam intensity (irradiance) as a function of distance from the mirror for different focal lengths. The solar irradiance at the surface of the earth on a clear sunny day is approximately  $0.1 \text{ W/cm}^2$ .

The plots in Figure 8 represent irradiance values that could be experienced at the eye at different distances and for mirrors of different focal lengths but with prescribed reflectivity, beam divergence angle, and effective mirror size. Eqs. (12) and (13) can be used to determine the beam irradiance ( $I$ , which is equivalent to  $E_c$  in Eq. (2)) for other mirror characteristics, and then Eqs. (1) and (2) can be used to determine the equivalent retinal irradiance for comparison against the safe retinal irradiance metrics in Figure 5.

#### 4.2 Analytical Model of Diffuse Reflections

Reflections from receivers, which are used to absorb the concentrated solar flux from heliostat, dish, and trough collector systems, can be modeled as diffuse rather than specular. Calculation of the irradiance at a location resulting from diffuse reflections depends on the total flux received by the source, reflectivity and size of the source, and distance to the source. First, the total power,  $P_d$  (W), emanating diffusely from the source is determined as follows:

$$P_d = 1000 C(A_d) \rho \quad (14)$$

where 1000 is the direct normal insolation ( $\text{W/m}^2$ ),  $C$  is the concentration ratio (Eq. (8)),  $A_d$  is the surface area of the diffuse source ( $\text{m}^2$ ), and  $\rho$  is the reflectivity of the diffuse source. For a diffuse source, we assume that the reflected radiation is spherically uniform in all directions, yielding the following equation for irradiance,  $E_{c,d}$  ( $\text{W/m}^2$ ) as a function of radial distance,  $r$  (m), from the source:

$$E_{c,d} = \frac{P_d}{A_r} = \frac{P_d}{4\pi r^2} \quad (15)$$

As an example, the irradiance from a diffusely reflecting power-tower receiver is calculated using the following parameters:

- Flux on power-tower receiver =  $1 \times 10^6 \text{ W/m}^2$  (1000 suns)
- Radius of receiver = 10 m
- Height of receiver = 20 m
- Receiver surface area =  $1,257 \text{ m}^2$  (calculated from receiver radius and height)
- Reflectivity of receiver = 0.1 – 0.5

Figure 9 shows a plot of the calculated irradiance as a function of distance from the receiver for reflectivity values of 0.1 and 0.5. The irradiance decreases rapidly with distance because the area over which the radiative power is distributed grows as a function of distance squared. The calculated irradiance can then be used to calculate the retinal irradiance (Eqs. (1) and (2)) for comparison against the safety metrics in Figure 5.

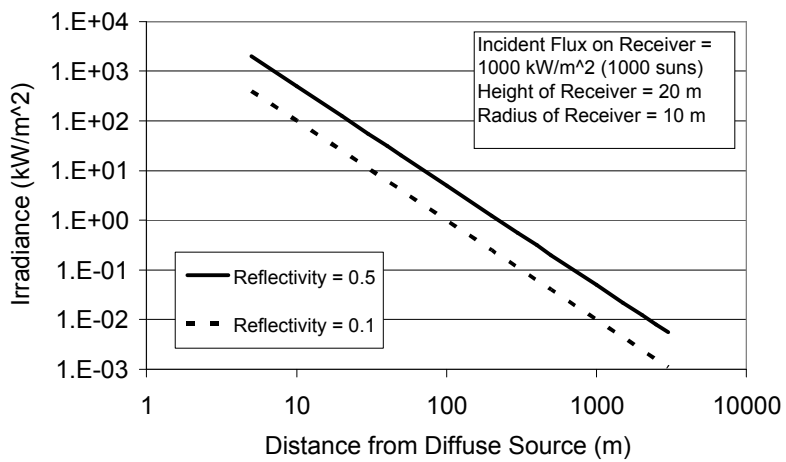


Figure 9. Irradiance as a function of distance from a diffuse source with different reflectivities.

#### 4.3 Computational Methods

The analytical methods described above provide convenient and quick calculations of irradiance from specularly or diffusely reflecting sources. Assumptions in these analytical models may potentially affect the accuracy of the calculated irradiance. For more accurate calculations of irradiance from reflecting surfaces, computational tools such as DELSOL, HELIOS, and ASAP<sup>®</sup> can be used [19]. As an example, a model was constructed in ASAP<sup>®</sup> (a ray-tracing code) to evaluate the irradiance on a 1 m<sup>2</sup> circular disk due to specular reflections from an off-axis parabolic dish. The reflections originated from the sun, where the elevation and azimuthal angles of the sun were determined from a prescribed latitude (34.96° N), Julian date (60) and solar hour (2 hours past solar noon). The sun shape and intensity distribution were taken from Rabl and Bendt [20] and incorporated into the model.

Figure 10 shows the geometry of the model and the simulated irradiance on the circular target for two different distances (all other parameters were the same). The red, blue, and green axes denote the x, y, and z directions, respectively, where west is in the +x direction, north is in the +z direction, and up is in the +y direction. For the prescribed latitude, date and time, the sun is located in the southwest quadrant of the domain. The top of Figure 10 shows the results for the closer distance, and the bottom of Figure 10 shows the results for the longer distance. At the longer distance, the simulated peak irradiance is significantly smaller than the peak irradiance at the closer distance (160 W/m<sup>2</sup> vs. 1100 W/m<sup>2</sup>). In addition, the size of the reflected sun image on the mirror is smaller at the larger distance. These results illustrate how computational models can be used to get accurate representations of the irradiance from specular or diffuse sources.

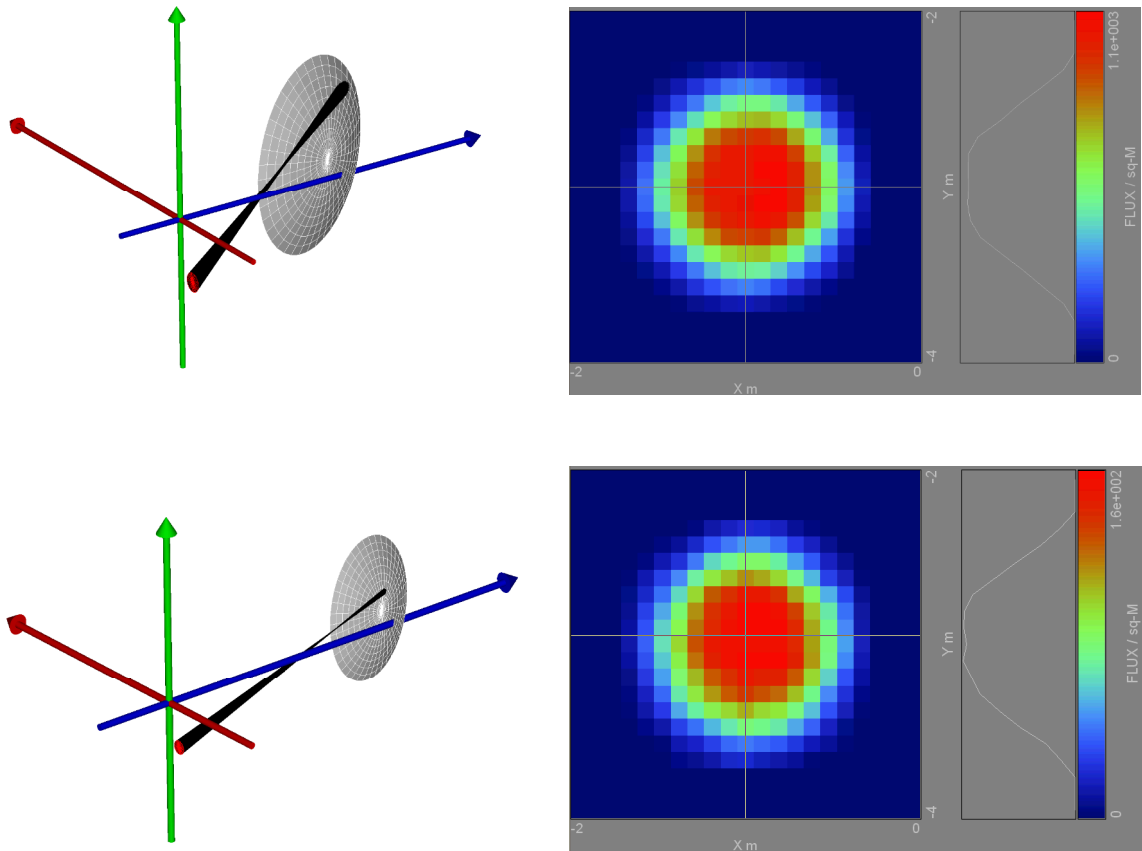


Figure 10. ASAP® model results. Diameter of dish = 10 m, focal length = 6 m, reflectivity = 0.94, parabolic shape, target location = (-1, -3, 0 m). Top: mirror location = (2, 0, **10** m), peak irradiance at target = 1100 W/m<sup>2</sup>. Bottom: mirror location = (2, 0, **20** m), peak irradiance at target = 160 W/m<sup>2</sup>.

## 5. Summary and Conclusions

This paper has presented methods to evaluate potential glint and glare hazards from specularly and diffusely reflected sunlight from concentrating solar collectors. First, a review of previous data and standards was performed to summarize metrics used to determine safe retinal irradiances as a function of subtended source angle (or retinal image size). These metrics were all based on preventing permanent eye damage, so a new metric that represents the potential for temporary flash blindness was introduced. The potential for temporary flash blindness can occur at irradiances several orders of magnitude lower than irradiances required for irreversible eye damage. Analytical models were then derived to calculate irradiances from both specular and diffuse sources. In addition, an example of irradiance calculations using a ray-tracing computational model was presented.

The methods and equations presented in this paper can be used to calculate irradiances from various concentrating solar collector systems (e.g., heliostats, dishes, troughs, receivers). These calculated irradiances can then be used to calculate the retinal irradiance using equations in Section 3.2. Finally, the calculated retinal irradiance can be compared against the safe retinal irradiance metrics provided in Section 3.3 to evaluate potential glint and glare hazards.

## Acknowledgments

The authors would like to thank Jim Adams from the California Energy Commission and Bill Kanemoto for pointing us to information relevant to glint and glare assessments in applications for certification.

Sandia is a multiprogram laboratory operated by Sandia Corporation, a Lockheed Martin Company for the

United States Department of Energy's National Nuclear Security Administration under contract DE-AC04-94AL85000. The United States Government retains and the publisher, by accepting the article for publication, acknowledges that the United States Government retains a non-exclusive, paid-up, irrevocable, world-wide license to publish or reproduce the published form of this manuscript, or allow others to do so, for United States Government purposes.

## References

- [1] Brumleve, T.D. (1977). Eye Hazard and Glint Evaluation for the 5-MW<sub>t</sub> Solar Thermal Test Facility, SAND76-8022, Sandia National Laboratories, Livermore, CA.
- [2] Brumleve, T.D. (1984). 10 MWe Solar Thermal Central Receiver Pilot Plant: Beam Safety Tests and Analyses, SAND83-8035, Sandia National Laboratories, Livermore, CA.
- [3] Sliney, D.H, and Freasier, B.C. (1973). Evaluation of Optical Radiation Hazards, *Applied Optics*, 12(1), 1-24.
- [4] Carrier, J. (2008). Beam Safety Design Parameters, Data Response Attachment DR89-1, Appendix A, Data Response Set 1A. Dated on 1/14/2008, CH2MHILL, Ivanpah Solar Electric Generating System, Application for Certification (07-AFC-5), Submitted to California Energy Commission, [http://www.energy.ca.gov/sitingcases/ivanpah/documents/applicant/DR\\_1a/2008-01-14\\_ISEGS\\_DR\\_SET\\_1A.PDF](http://www.energy.ca.gov/sitingcases/ivanpah/documents/applicant/DR_1a/2008-01-14_ISEGS_DR_SET_1A.PDF).
- [5] Carrizo Energy, LLC (2008). Responses to CEC Data Requests (#1-78), Application for Certification (07-AFC-8), Carrizo Energy Solar Farm, Submitted to California Energy Commission, [http://www.energy.ca.gov/sitingcases/carrizo/documents/applicant/2008-02-27\\_DATA\\_RESPONSES\\_1-78.PDF](http://www.energy.ca.gov/sitingcases/carrizo/documents/applicant/2008-02-27_DATA_RESPONSES_1-78.PDF).
- [6] City of Victorville, (2008). Victorville 2 Hybrid Power Project, Application for Certification (07-AFC-1), submitted to California Energy Commission, [www.energy.ca.gov/sitingcases/victorville2/documents/](http://www.energy.ca.gov/sitingcases/victorville2/documents/).
- [7] San Joaquin Solar 1 & 2 – Application for Certification Volume 2, Appendix L, “Glint and Glare Study,” [http://www.energy.ca.gov/sitingcases/sjsolar/documents/applicant/afc/afc\\_volume\\_02/](http://www.energy.ca.gov/sitingcases/sjsolar/documents/applicant/afc/afc_volume_02/).
- [8] SES Solar Two, LLC (2008). SES Solar Two Project, Application for Certification (08-AFC-5), submitted to California Energy Commission.
- [9] Ghanbari, C.M. and Diver, R.B. (1994). Glint Hazard Assessment, Sandia National Laboratories Internal Memo, April 21, 1994.
- [10] American Conference of Governmental Industrial Hygienists (ACGIH) (1992-1993). Threshold Limit Values for Chemical Substances and Physical Agents.
- [11] Sliney, D.H., (1980). An Evaluation of the Potential Hazards of the Point Focusing Solar Concentrators at the JPL-Edwards Test Site, Report submitted to the Jet Propulsion Laboratory (JPL Consulting Agreement No. JF 714696), California Institute of Technology, Pasadena, CA.
- [12] Hoover, H.L., (1986). Solar ultraviolet irradiation of human cornea, lens, and retina: equations of ocular irradiation.
- [13] Osterhaus, W.K.E., (2005). Discomfort glare assessment and prevention for daylight applications in office environments, *Solar Energy*, 79, 140-158.
- [14] Iwata, T. and K. Kimura, (1990/1991). Discomfort Caused by Wide-source Glare, *Energy and Buildings*, 15-16, 391-398.
- [15] Delori, F.C., R.H. Webb, and D.H. Sliney, (2007). Maximum permissible exposures for ocular safety (ANSI 2000), with emphasis on ophthalmic devices, *J. Opt. Soc. Am. A*, 24(5), 1250-1265.
- [16] Metcalf, R.D and R.E. Horn, (1958). Visual Recovery Times from High-Intensity Flashes of Light, *Air Force Aerospace Medical Research Lab, Wright Air Development Center Technical Report 58232*.

- [17] Severin, S.L. N.L. Newton, and J.F. Culver, (1962). An Experimental Approach to Flash Blindness, *Aerospace Medicine*, 1199-1205.
- [18] Saur, R.L. and S.M. Dobrash, (1969). Duration of Afterimage Disability after Viewing Simulated Sun Reflections, *Applied Optics*, 8(9), 1799-1801.
- [19] Ho, (2008). Software and Codes for Analysis of Concentrating Solar Power Technologies, SAND2008-8053, Sandia National Laboratories, Albuquerque, NM.  
[http://infoserve.sandia.gov/sand\\_doc/2008/088053.pdf](http://infoserve.sandia.gov/sand_doc/2008/088053.pdf)
- [20] Rabl, A. and P. Bendt, (1982). Effect of Circumsolar Radiation on Performance of Focusing Collectors, *J. Solar Energy Engineering*, 104, 237-250.
- [21] Duffie, J.A. and W.A. Beckman, (1991) Solar Engineering of Thermal Processes, 2<sup>nd</sup> Ed., John Wiley & Sons, Inc., New York.

### Appendix: Sample Calculations Using ACGIH Threshold Limit Values

Proposed exposure limits for optical radiation have been published by the American Conference of Governmental Industrial Hygienist (ACGIH) [10]. These limits are called Threshold Limit Values (TLVs) and are calculated from spectrally weighted radiometric values of radiance or irradiance. TLVs are evaluated for (1) retinal thermal damage, (2) photochemical injury from chronic blue light exposure, (3) and infrared radiation damage.

A screen image of an Excel spreadsheet created to evaluate the ACGIH TLVs is provided in Figure 11. These calculations are intended to provide conservative estimates of a “worst case” hazard from the Cummins Power Generation, Inc. CPG-460 dish. For this example, we assume that the flux “hot spot” is focused on the aperture plate, outside of the receiver’s aperture, and that it is 0.2 meters in diameter and has an intensity of 600 W/cm<sup>2</sup>. The target irradiance,  $I_t$ , (W/cm<sup>2</sup>) is based on the incident solar intensity and the target reflectance,  $\rho$ . The target reflectance is assumed to be gray and 0.5 in this example ( $I_t = 600 \text{ W/cm}^2 \times 0.5 = 300 \text{ W/cm}^2$ ). To simplify the calculations, we assume that the target is a gray, diffuse reflector, that there are no cosine effects, and that the intensity is uniform over the entire surface of the circular target of radius  $r$  ( $r = 0.1$  meters in the example). A consequence of these simplifying (and conservative) assumptions is that the target can be considered to be a hemisphere of radius  $r$ , with a uniform intensity of  $I_t$ . The irradiance at a distance  $d$  from the target,  $I_d$ , is then  $I_t(r^2/d^2)$ . The assumptions used in the model are listed below.

- The target surface is a gray, diffuse reflector
- There are no cosine effects
- The incident solar flux is uniform over the surface of the target
- The incident solar flux on the target is 600 W/cm<sup>2</sup> in the example
- The target reflectance is 0.5 in the example
- The diameter of the target is 0.2 meters in the example
- The retinal irradiance is evaluated at 5, 10, 15 and 20 meters away from the target.

Radiance,  $L$ , (W/cm<sup>2</sup> sr<sup>-1</sup>) is defined as irradiance divided by the solid angle subtended by the source. Therefore for spectral radiance,  $L_\lambda$ , we divide spectral irradiance by the solid angle (steradians) subtended by the source. We assume that the spectral distribution from the target is proportional to the extraterrestrial spectral solar irradiance,  $E_\lambda$ , given in Duffie and Beckman [21], averaged over small bandwidths centered at various values of  $\lambda$ . These bandwidths correspond to the ACGIH bandwidths for spectral weighting functions. To calculate  $L_\lambda$ , the spectral radiance at the wavelength  $\lambda$ , we use the irradiance value (normalized to one sun (0.1 W/cm<sup>2</sup>)) calculated at each distance from the source,  $I_d$ , multiply it by  $E_\lambda$  and 1000/1353 (to scale it for terrestrial solar intensity) and then divide that quantity by the solid angle subtended

by the source at the same distance ( $\alpha$ ).

$$L_\lambda = \left( \frac{I_d}{0.1} \bullet E_\lambda \bullet \frac{1000}{1353} \right) / \alpha \quad (16)$$

The value for  $L_\lambda$  at each  $\lambda$  is the same regardless of the distance. This is because radiance is defined as: “the radiometric equivalent of luminance or “brightness,” a quantity that does not vary with viewing distance. For example, the irradiance from a diffused lamp bulb decreases as the inverse square of the distance and proportionally less light enters the eye. However, the retinal area of the light bulbs image also decreases as the inverse square of the distance, so that the retinal irradiance for an extended source stays constant with distance.” [10]

### Retinal Thermal Damage

Thermal injury to the retina is dependent on the time-temperature history of the heated tissue. Brumleve [1] and Sliney [11] calculated retinal irradiance of direct ocular viewing of the sun of 8.5 and 4.5 to 7.0 W/cm<sup>2</sup>, respectively. By comparison, the calculated retinal irradiance of viewing the target in the example is 0.5 W/cm<sup>2</sup>. ACGIH TLVs are a function of exposure time and are spectrally weighted by ACGIH indices. The following expression is used to calculate retinal thermal damage TLVs.

$$\sum_{400}^{1400} L_\lambda \bullet R_\lambda \bullet \Delta\lambda \leq 1/(\alpha t^{1/2}) \quad (17)$$

Where:

- $\lambda$  varies between 400 and 1400 nm (the transmission band of the eye)
- $R_\lambda$  is the ACGIH spectral weighting function for retinal thermal damage
- $L_\lambda$  is calculated as shown in Eq. (16)
- $t$  is the viewing time in seconds

Assuming a condition of equality for Eq. (17), we can solve for  $t$  (the maximum allowable viewing time). For the range of distances considered, 5 to 20 meters, the viewing times vary from 0.03 seconds at 5 meters to 0.53 seconds at a distance of 20 meters. As one would expect, the closer an observer is to the source the shorter the viewing time must be. These short allowable viewing times are a result of the relatively large subtended angles of the source (0.04 rad at 5 m and 0.01 rad at 20 m).

### Retinal Photochemical Injury

The second area of concern is retinal photochemical injury from chronic exposure to short wavelength (blue) light. The following equations are used to evaluate this hazard which is also known as the blue-light hazard.

$$\sum_{400}^{700} L_\lambda \bullet t \bullet B_\lambda \bullet \Delta\lambda \leq 100 \text{ J/cm}^2\text{-sr} \quad (t \leq 10^4 \text{ sec}) \quad (18)$$

$$\sum_{400}^{700} L_\lambda \bullet B_\lambda \bullet \Delta\lambda \leq 0.01 \text{ W/cm}^2\text{-sr} \quad (t \geq 10^4 \text{ sec}) \quad (19)$$

According to the ACGIH, the weighted product of  $L_\lambda$  and  $B_\lambda$  is termed  $L$  (blue).  $B_\lambda$  in Eqs. (18) and (19) is the ACGIH spectral weighting function for blue-light hazard. For a source radiance  $L$  weighted against the blue-light hazard function,  $L$  (blue), which exceeds 10 mW cm<sup>-2</sup> sr<sup>-1</sup> in the blue spectral region, the permissible exposure duration  $t_{\max}$  in seconds is simply:

$$t_{\max} = 100 \text{ J} \cdot \text{cm}^{-2} / L(\text{blue}) \quad (20)$$

By solving Eq. (20), we find that the maximum allowable viewing time in the example is 11 seconds. For light sources that subtend an angle less than 0.011 radians, a different set of equations is used. At 15 m and

20 m in the example (as well as larger distances), the subtended angle of the light source (target) is less than 0.011 radians and the following equations apply.

$$\sum_{400}^{700} E_\lambda \cdot t \cdot B_\lambda \cdot \Delta\lambda \leq 10 \text{ mJ/cm}^2 \quad (t \leq 10^4 \text{ sec}) \quad (21)$$

and

$$\sum_{400}^{700} E_\lambda \cdot B_\lambda \cdot \Delta\lambda \leq 1 \text{ } \mu\text{W/cm}^2 \quad (t \geq 10^4 \text{ sec}) \quad (22)$$

Again, we can solve for the maximum allowable viewing time by the following equation:

$$t_{\max} = 10 \text{ mJ} \cdot \text{cm}^{-2} / E(\text{blue}) \quad (23)$$

where  $E(\text{blue})$  is the weighted product of  $E_\lambda$  and  $B_\lambda$ . The times were determined to be 8 and 11 seconds at 15 and 20 meters, respectively.

### **Infrared Radiation Damage**

The third area of concern is infrared radiation. The ACGIH index states “To avoid possible delayed effects upon the lens of the eye (cataractogenesis), the infrared radiation ( $\lambda=770$  nm) should be limited to 10 mW/cm<sup>2</sup>. For an infrared heat lamp or any near-infrared source where a strong visual stimulus is absent, the near-infrared (770-1400 nm) radiance as viewed by the eye should be limited to:

$$\sum_{770}^{1400} L_\lambda \cdot \Delta\lambda \leq 0.6 / \alpha \quad (24)$$

for extended duration viewing conditions.” For the viewing distances evaluated, the left hand side of the equation is much less than the right hand side. In addition, because there is a strong visual stimulus, this should not be an area of concern.

Assumptions									
Peak flux (W/cm <sup>2</sup> )									600
Reflectivity									0.5
Target Diameter(m)									0.2
<b>I2 - intensity (W/cm<sup>2</sup>)</b>	5	10	15	20					<b>Beam Radiance, <math>L_i</math> (W/cm<sup>2</sup>sr)</b>
300	1.20E-01	3.00E-02	1.33E-02	7.50E-03					5m 10m 15m 20m
Suns ->	1.20E+00	3.00E-01	1.33E-01	7.50E-02					95.53 95.50 95.50 95.50
<b>Alpha - Angle subtended from point on ground to target</b>									
(degrees)	5m	10m	15m	20m					<b>Retinal Irradiance, <math>E_r</math> (W/cm<sup>2</sup>)</b>
(radians)	0.04	0.02	0.0133E-02	0.001E-02					5m 10m 15m 20m
(sterrad)	1.26E-03	3.14E-04	1.40E-04	7.85E-05					0.50 0.50 0.50 0.50
Wave Length (W/m <sup>2</sup> sr.um)	E-lamda	R(lamda)	Spec Rad L-lamda	L*R* L(blue) $\Delta\lambda$	E(blue) 15m	E(blue) 20m			<b>InfraRed L'del-lamda (W/cm<sup>2</sup>sr-nm)</b>
(nm)	(ACGIH)	(W/cm <sup>2</sup> sr-nm)							
			<b>@5m</b>	<b>@5m</b>					
395									
400	1,429	1.00	1.01E-01	0.50 0.050449	7.04114E-06	5.35875E-06			--
405	1,590	2.00	1.12E-01	1.12 0.112265	1.56689E-05	0.000011925			--
410	1,751	4.00	1.24E-01	2.47 0.247265	3.4511E-05	0.000026265			--
415	1,749	8.00	1.23E-01	4.94 0.493966	6.89431E-05	0.00005247			--
420	1,747	9.00	1.23E-01	5.55 0.555076	7.74723E-05	5.89613E-05			--
425	1,693	9.50	1.20E-01	5.68 0.567803	7.92486E-05	6.03131E-05			--
430	1,639	9.80	1.16E-01	5.67 0.567051	7.91436E-05	6.02333E-05			--
435	1,725	10.00	1.22E-01	6.09 0.608808	8.49717E-05	6.46688E-05			--
440	1,810	10.00	1.28E-01	6.39 0.638993	8.91845E-05	0.000067875			--
445	1,908	9.70	1.35E-01	6.53 0.653382	9.11929E-05	6.94035E-05			--
450	2,006	9.40	1.42E-01	6.66 0.665696	9.29116E-05	7.07115E-05			--
455	2,036	9.00	1.44E-01	6.47 0.646901	9.02882E-05	0.000068715			--
460	2,066	8.00	1.46E-01	5.83 0.583496	8.14388E-05	0.00006198			--
465	2,050	7.00	1.45E-01	5.06 0.506481	7.06898E-05	5.37994E-05			--
470	2,033	6.20	1.44E-01	4.45 0.444986	6.21069E-05	4.72673E-05			--
475	2,054	5.50	1.45E-01	3.99 0.398726	5.56504E-05	4.23534E-05			--
480	2,074	4.50	1.46E-01	3.29 0.329487	4.59867E-05	3.49988E-05			--
485	2,012	4.00	1.42E-01	2.84 0.284122	3.96551E-05	0.00003018			--
490	1,950	2.20	1.38E-01	1.51 0.151452	2.11382E-05	1.60875E-05			--
495	1,946	1.60	1.37E-01	1.10 0.109921	1.53417E-05	0.000011676			--
500	1,942	1.00	1.37E-01	0.69 0.068559	9.56886E-06	7.2825E-06			--
510	1,882	1.00	1.33E-01	1.33 0.083843	1.1702E-05	8.90596E-06			--
520	1,833	1.00	1.29E-01	1.29 0.051524	7.19123E-06	5.47298E-06			--
530	1,842	1.00	1.30E-01	1.30 0.032669	4.55964E-06	3.47017E-06			--
540	1,783	1.00	1.26E-01	1.26 0.019953	2.78479E-06	2.1194E-06			--
550	1,725	1.00	1.22E-01	1.22 0.01218	1.69993E-06	1.29375E-06			--
560	1,695	1.00	1.20E-01	1.20 0.007551	1.05393E-06	8.02105E-07			--
570	1,712	1.00	1.21E-01	1.21 0.004812	6.71653E-07	5.1117E-07			--
580	1,715	1.00	1.21E-01	1.21 0.003042	4.24527E-07	3.23091E-07			--
590	1,700	1.00	1.20E-01	1.20 0.001902	2.65515E-07	2.02074E-07			--
600	1,666	1.00	1.18E-01	1.18 0.001176	1.64178E-07	1.2495E-07			--
620	1,602	1.00	1.13E-01	2.26 0.002262	3.15743E-07	2.403E-07			--
640	1,544	1.00	1.09E-01	2.18 0.00218	3.04311E-07	2.316E-07			--
660	1,486	1.00	1.05E-01	2.10 0.002098	2.9288E-07	2.229E-07			--
680	1,427	1.00	1.01E-01	2.02 0.002015	2.81252E-07	2.1405E-07			--
700	1,369	1.00	9.67E-02	1.93 0.001933	2.6982E-07	2.0535E-07			--
720	1,314	1.00	9.28E-02	1.86					--
750	1,235	1.00	8.72E-02	2.62					2.616
800	1,109	1.00	7.83E-02	3.92	Photochemical Injury from Chronic Blue Light Exposure				3.915
900	891	1.00	6.29E-02	6.29	For Sources subtending >0.011 rad				6.291
1000	748	1.00	5.28E-02	5.28	For Sources subtending >0.011 rad				5.281
1200	485	1.00	3.42E-02	6.85	$\sum_{400}^{700} L_{\lambda} \cdot t \cdot B_{\lambda} \cdot \Delta\lambda \leq 100 \text{ J / cm}^2 \cdot \text{sr}$ (t $\leq 10^4$ s)				6.849
1400	337	0.20	2.38E-02	0.95	$\sum_{400}^{700} L_{\lambda} \cdot t \cdot B_{\lambda} \cdot \Delta\lambda \leq 100 \text{ J / cm}^2 \cdot \text{sr}$ (t $\leq 10^4$ s)				4.759
<b>Retinal Thermal Injury</b>									
<b>Equation 1</b>									
$\sum_{400}^{700} L_{\lambda} \cdot R_{\lambda} \cdot \Delta\lambda = 1 / (\alpha \sqrt{t})$									
Solving for equation1, the maximum viewing time at each distance is :									
viewing time	5m	10m	15m	20m					
	0.03	0.13	0.30	0.53					
The solid angle depends on the distance									
$\sum_{400}^{700} E_{\lambda} \cdot t \cdot B_{\lambda} \cdot \Delta\lambda \leq 10 \text{ mJ / cm}^2 \cdot \text{sr}$ (t $\leq 10^4$ s)									
$\sum_{400}^{700} E_{\lambda} \cdot B_{\lambda} \cdot \Delta\lambda \leq 1 \mu\text{W} / \text{cm}^2 \cdot \text{sr}$ (t $\leq 10^4$ s)									
maximum viewing time									
$t_{\max} = 10 \text{ mJ} \cdot \text{cm}^{-2} / E_{\text{blue}}$									
$E_{\text{blue}} = \frac{15\text{m}}{1.24\text{E-03}} \quad \frac{20\text{m}}{9.47\text{E-04}}$ W/cm <sup>2</sup>									
$t_{\max} = \frac{8.04}{1.24\text{E-03}} \quad \frac{10.56 \text{ seconds}}{9.47\text{E-04}}$									
For Infrared									
$\sum_{700}^{1000} L_{\lambda} \cdot \Delta\lambda \leq 0.6 / \alpha$									
the rhs for various distances is:									
5m 15.00									
10m 30.00									
15m 45.00									
20m 60.00									

Figure 11. Excel® worksheet to calculate ACGIH TLVs.